

## A fluorescent layered oxalato-based canted antiferromagnet

Samia Benmansour,<sup>\*a</sup> Christian Cerezo-Navarrete,<sup>a</sup> Josep Canet-Ferrer,<sup>ab</sup> Guillermo Muñoz-Matutano,<sup>c</sup> Juan Martínez-Pastor<sup>c</sup> and Carlos J. Gómez-García<sup>\*a</sup>

<sup>a</sup>Instituto de Ciencia Molecular (ICMol), Parque Científico, Universidad de Valencia, C/ Catedrático José Beltrán, 2, 46980 Paterna (Valencia), Spain.

<sup>b</sup>ICFO – Institut de Ciències Fotòniques, the Barcelona Institute of Science and Technology, 08860 Barcelona, Spain.

<sup>c</sup>Instituto de Ciencia de los Materiales (ICMUV), Universidad de Valencia, C/ Catedrático José Beltrán, 2, 46980 Paterna (Valencia), Spain.

### Supporting Information

#### Powder X-ray Diffraction analysis (PXRD)

The phase purity of compound **1** was confirmed by comparing its experimental powder X-ray diffraction pattern with the simulated one from the single crystal X-ray structure determination (Figure S1).

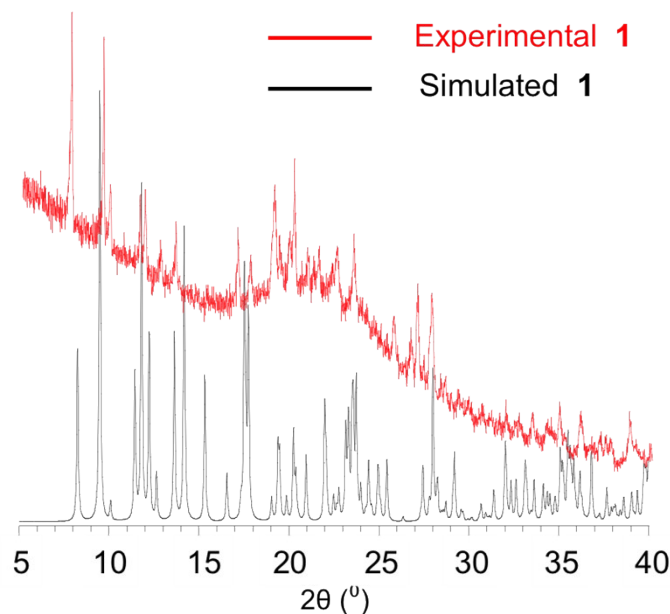


**Figure S1.** Experimental and simulated X-ray powder diffractogram for compound [DOC][MnFe(C<sub>2</sub>O<sub>4</sub>)<sub>3</sub>] (**1**) (DOC = 3,3'-Diethyloxacarbocyanine).

**Table S1.** Main bond distances ( $\text{\AA}$ ) for compound [DOC][MnFe(C<sub>2</sub>O<sub>4</sub>)<sub>3</sub>] (**1**).

<b>Atoms</b>	<b>distance (<math>\text{\AA}</math>)</b>	<b>Atoms</b>	<b>distance (<math>\text{\AA}</math>)</b>	<b>Atoms</b>	<b>distance (<math>\text{\AA}</math>)</b>	<b>Atoms</b>	<b>distance (<math>\text{\AA}</math>)</b>
M1-O1	2.080(5)	M11-O13	2.067(5)	C1-O1	1.246(8)	C3-O5	1.251(7)
M1-O3	2.085(5)	M11-O11	2.082(5)	C2-O2	1.256(8)	C4-O6	1.256(8)
M1-O6 <sup>#1</sup>	2.097(5)	M11-O14	2.083(5)	C1-O11	1.254(8)	C3-C4	1.549(10)
M1-O2	2.098(5)	M11-O15 <sup>#2</sup>	2.091(5)	C2-O12	1.259(8)	C13-O13	1.250(8)
M1-O5 <sup>#1</sup>	2.100(5)	M11-O16 <sup>#2</sup>	2.101(5)	C1-C2	1.565(9)	C14-O14	1.256(8)
M1-O4	2.120(5)	M11-O12	2.101(5)	C3-O3	1.253(8)	C13-O15	1.265(8)
				C4-O4	1.251(8)	C14-O16	1.258(8)
						C13-C14	1.533(10)

M = Mn/Fe (50 % each)

Symmetry transformations to generate equivalent atoms: #1 = x, -y+1/2, z+1/2; #2 = x, -y+3/2, z+1/2

**Table S2.** Main bond angles ( $^{\circ}$ ) for compound [DOC][MnFe(C<sub>2</sub>O<sub>4</sub>)<sub>3</sub>] (**1**).

<b>Atoms</b>	<b>angle (<math>^{\circ}</math>)</b>	<b>Atoms</b>	<b>angle (<math>^{\circ}</math>)</b>
O1-M1-O3	164.20(19)	O13-M11-O11	169.6(2)
O1-M1-O6 <sup>#1</sup>	94.94(18)	O13-M11-O14	79.45(19)
O3-M1-O6 <sup>#1</sup>	95.57(18)	O11-M11-O14	92.93(19)
O1-M1-O2	79.69(18)	O13-M11-O15 <sup>#2</sup>	91.4(2)
O3-M1-O2	91.15(18)	O11-M11-O15 <sup>#2</sup>	97.23(19)
O6 <sup>#1</sup> -M1-O2	171.26(19)	O14-M11-O15 <sup>#2</sup>	166.67(19)
O1-M1-O5 <sup>#1</sup>	101.06(18)	O13-M11-O16 <sup>#2</sup>	95.50(18)
O3-M1-O5 <sup>#1</sup>	92.59(19)	O11-M11-O16 <sup>#2</sup>	91.74(18)
O6 <sup>#1</sup> -M1-O5 <sup>#1</sup>	78.42(18)	O14-M11-O16 <sup>#2</sup>	91.79(19)
O2-M1-O5 <sup>#1</sup>	95.74(18)	O15 <sup>#2</sup> -M11-O16 <sup>#2</sup>	79.34(19)
O1-M1-O4	88.53(18)	O13-M11-O12	94.89(19)
O3-M1-O4	79.44(18)	O11-M11-O12	79.67(19)
O6 <sup>#1</sup> -M1-O4	91.50(18)	O14-M11-O12	101.84(19)
O2-M1-O4	95.22(18)	O15 <sup>#2</sup> -M11-O12	88.50(19)
O5 <sup>#1</sup> -M1-O4	166.56(18)	O16 <sup>#2</sup> -M11-O12	164.17(19)

M = Mn/Fe (50 % each)

Symmetry transformations to generate equivalent atoms: #1 = x, -y+1/2, z+1/2; #2 = x, -y+3/2, z+1/2

### Shape analysis of the coordination geometries of Fe1 and Mn1

The analysis with the program SHAPE<sup>1</sup> of the coordination geometries of the Er ions in the six compounds is summarized in table S2.

**Table S3.** SHAPE values for the 5 possible coordination geometries found for coordination number six<sup>2</sup> in compound [DOC][MnFe(C<sub>2</sub>O<sub>4</sub>)<sub>3</sub>] (**1**).

Geometry	symmetry	Fe1	Mn1
HP-6	D <sub>6h</sub>	31.762	32.476
PPY-6	C <sub>5v</sub>	23.988	23.638
OC-6	O <sub>h</sub>	<b>1.336</b>	<b>1.395</b>
TPR-6	D <sub>3h</sub>	10.945	10.457
JPPY-6	C <sub>5v</sub>	27.685	27.413

HP-6 = hexagon; PPY-6 = pentagonal pyramid;

OC-6 = octahedron; TPR-6 = trigonal prism;

JPPY-6 = Johnson pentagonal pyramid J2.

The minima values are indicated in bold.

### Magnetic properties

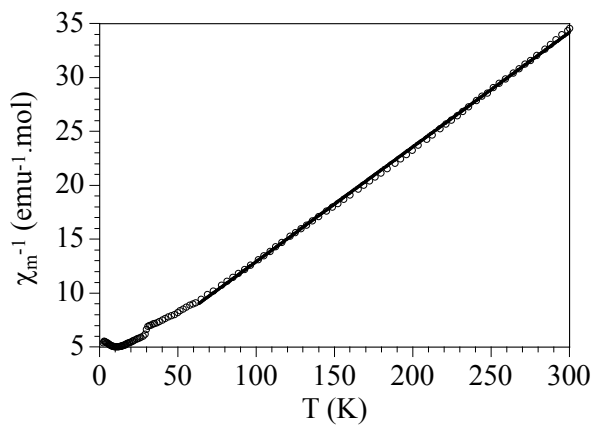


**Figure S2.** Curie-Weiss plot of compound [DOC][MnFe(C<sub>2</sub>O<sub>4</sub>)<sub>3</sub>] (**1**). Solid line is the best fit to the Curie-Weiss law of the high temperature region, with C = 9.4 cm<sup>3</sup> K mol<sup>-1</sup> and θ = -21.8 K.

Since the expected saturation magnetization value for a parallel alignment of the two S = 5/2 spins is *ca.* 10 μ<sub>B</sub>, then, the smooth saturation of *ca.* 0.015 μ<sub>B</sub> observed in the isothermal magnetization of compound **1** at 2 K indicates that the canting angle (α) between the two S = 5/2 spins is: tan α = 0.015/10 = 0.0015. This means that α ≈ 0.1°.

## Luminescent properties

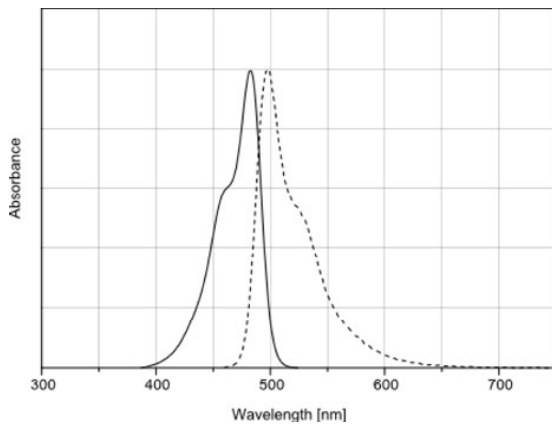


**Figure S3.** Absorption spectrum (continuous line) and emission spectrum (dashed line) of the dye (DOC)I in methanol. (Absorption maximum = 483 nm, fluorescence maximum = 498 nm, data provided by the dye manufacturer: Few Chemicals)

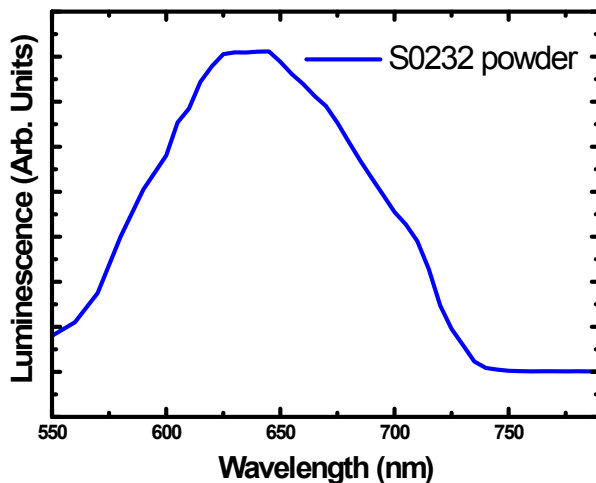


**Figure S4.** Luminescence spectrum of crystals of the dye (DOC)I measured with similar excitation power conditions than compound **1**.

## Luminescent properties at low temperature

At low temperatures (12 K) the sample emission is affected by a background arising from the impurities of the quartz wafer (Figure S5). These impurities are more active at the near-infrared, so at the visible region the emission spectrum is still dominated by the  $\text{DOC}^+$  dye emission. The same three bands observed at room temperature (P1, P2 and P3 in Figure 5) are found at the same wavelengths, within the experimental error of the Gaussian fit and background de-convolution. Indeed, after removing the contribution of the quartz impurities (grey line), the obtained spectrum (dashed purple line) is very similar to the one observed at room temperature.

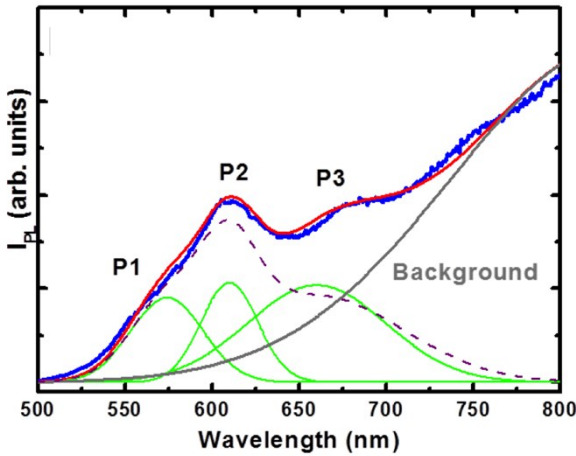


**Figure S5:** Fluorescence spectra at 12 K of a polycrystalline sample of compound **1** (blue line). P1, P2 and P3 are the Gaussian components (green lines) corresponding to the best fit of the experimental spectra (red lines). The purple dashed line is the resulting spectrum after subtracting the background contribution associated to the emission of the quartz wafer impurities (grey line).

## IR spectra

The IR spectrum of compound [DOC][MnFe(C<sub>2</sub>O<sub>4</sub>)<sub>3</sub>] (**1**) (Figure S6) shows the bands observed in the iodide salt of the dye (DOC)I (Figure S7) plus some bands associated to the oxalato layer. The assignments<sup>3</sup> of the main bands are shown in table S4. Figure S8 shows both spectra in the same plot.

**Table S4.** Main IR band and their assignments in compounds [DOC][MnFe(C<sub>2</sub>O<sub>4</sub>)<sub>3</sub>] (**1**) and (DOC)I.

Band	(DOC)I <sup>a</sup>	(DOC)I <sup>b</sup>	<b>1</b>
v (C=O) <sub>bridge</sub>	-	-	1636
v (C-H)sp <sup>2</sup>	1567	1564	1568
	1508	1506	1510
	1453	1457	1457
v(ArC-H)	1633	1630	1636 <sup>c</sup>
	1610	1609	
δ(C-H)sp <sup>3</sup>	1476	1477	1479
δ(C-H)sp <sup>2</sup>	756	767	752
	738	736	

<sup>a</sup> Data from reference 3. <sup>b</sup> Data from the precursor salt (DOC)I from Few Chemicals.

<sup>c</sup> Overlapping with the oxalato stretching C=O vibration.

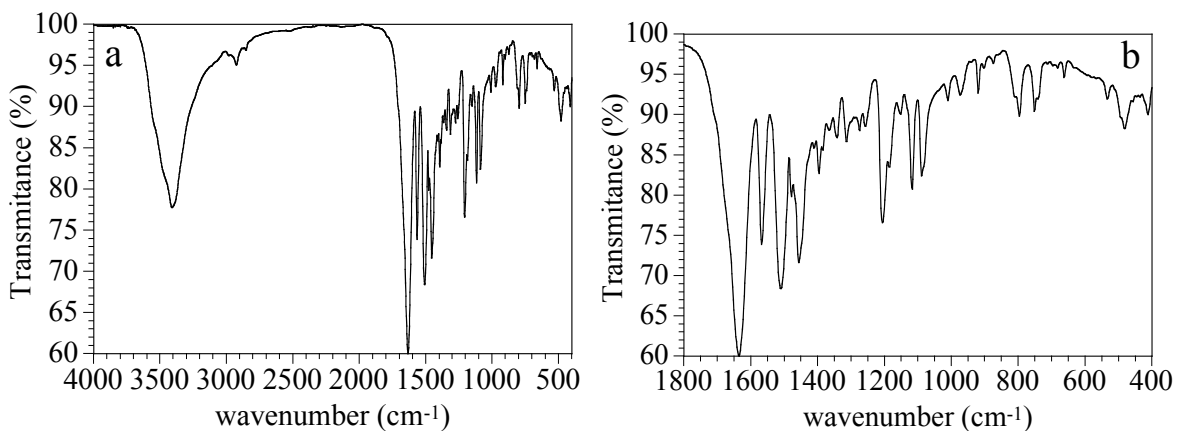


**Figure S6.** IR spectrum of compound [DOC][MnFe(C<sub>2</sub>O<sub>4</sub>)<sub>3</sub>] (**1**) in **(a)** the 4000-400 cm<sup>-1</sup> range and **(b)** 1800-400 cm<sup>-1</sup> range.

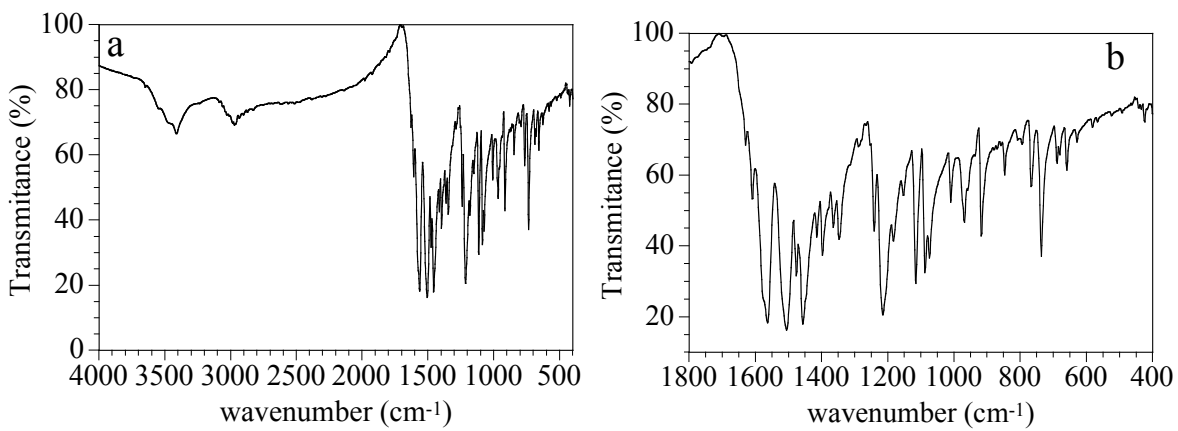


**Figure S7.** IR spectrum of compound (DOC)I in **(a)** the 4000-400 cm<sup>-1</sup> range and **(b)** 1800-400 cm<sup>-1</sup> range.

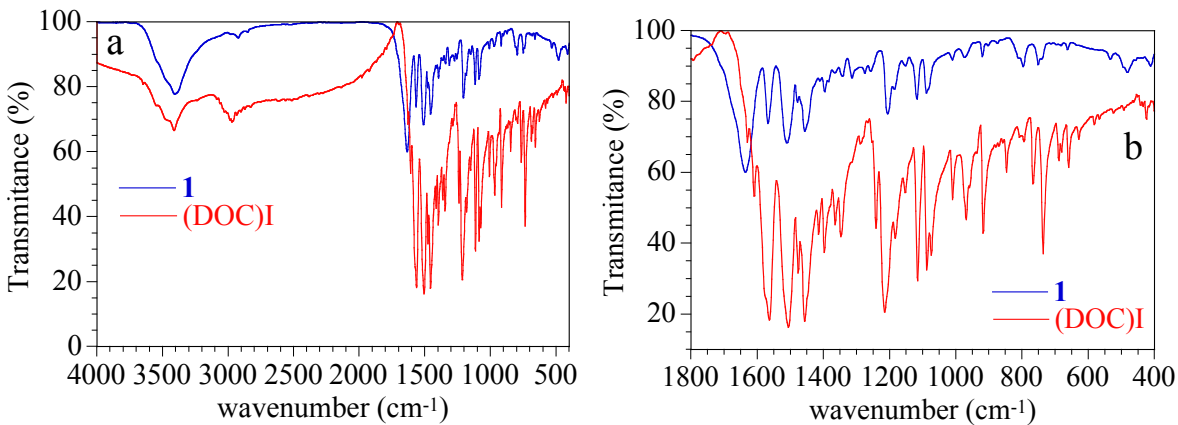


**Figure S8.** IR spectra of compounds **1** and (DOC)I in **(a)** the 4000-400 cm<sup>-1</sup> range and **(b)** 1800-400 cm<sup>-1</sup> range.

## References

- 1-Llunell, M.; Casanova, D.; Cirera, J.; Bofill, J. M.; Alemany, P.; Alvarez, S.; Pinsky, M.; Avnir, D. SHAPE, version 2.3, University of Barcelona, Barcelona, Spain, and Hebrew University of Jerusalem, Jerusalem, Israel, **2013**.
- 2-Alvarez, S.; Avnir, D.; Llunell, M.; Pinsky, M. Continuous symmetry maps and shape classification. The case of six-coordinated metal compounds. *New J. Chem.* **2002**, *26*, 996-1009.
- 3-Leifer, A.; Bonis, D.; Boedner, M.; Dougherty, P.; Fusco, A. J.; Koral, M.; LuValle, J. E. Investigation of Spectral Sensitization V. A Study of the Visible and Infrared Spectra of Some Very Pure 2-bis-Benzoxazolyl, 2-bis-Indolinyl, and 2-bis-Quinolyl Cyanine Iodides. *Appl. Spectrosc.* **1967**, *21*, 71-80.